The Binding of Benzoarylsulfonamide Ligands to Human Carbonic Anhydrase is Insensitive to Formal Fluorination of the Ligand

Permanent link

Terms of Use

Share Your Story

The Binding of Benzoarylsulfonamide Ligands to Human Carbonic Anhydrase is Insensitive to Formal Fluorination of the Ligand

Heiko Lange,[a,†] Matthew R. Lockett,[a,†] Benjamin Breiten,[a] Annie Heroux,[b] Woody Sherman,[c]

Dmitrij Rappoport,[a] Patricia O. Yau,[a] Philip W. Snyder,[a] George M. Whitesides[a,d,*]

[a] Department of Chemistry and Chemical Biology, Harvard University
12 Oxford Street, Cambridge, MA 02138

[b] National Synchrotron Light Source, Brookhaven National Laboratory
725 Brookhaven Avenue, Upton, NY 11973

[c] Schrödinger Inc.
120 West 45th Street, New York, NY 10036

[d] Wyss Institute for Biologically Inspired Engineering, Harvard University
60 Oxford Street, Cambridge, MA 02138

* Author to whom correspondence should be addressed: gwhitesides@gmwgroup.harvard.edu

[†] These authors contributed equally.

The hydrophobic effect (or the aggregated *effects* that we call "the hydrophobic effect") underlies the binding of many ligands to proteins. It involves three molecular participants: the surface of the binding pocket of the protein, the surface of the ligand, and the networks of water molecules that fill the pocket and surround the ligand. The molecular-level mechanism of the hydrophobic effect in protein-ligand binding remains a subject of substantial controversy.[1, 2] There are three primary questions of interest: i) "Do hydrophobic effects reflect the release of structured, and hence entropically unfavorable, water from hydrophobic surfaces when the ligand and surface of the binding pocket come into contact?"; ii) "Do hydrophobic effects represent the release of free-energetically unfavorable water from hydrogen-bonded networks in the binding pocket or displacement by the ligand, and the release of free-energetically unfavorable (although perhaps different) waters from the hydrophobic surface of the ligand?"; and iii) "How important in free energy are the contact interactions between the protein and the ligand in the binding pocket?".

In a previous examination of these questions,[3] we compared the binding of a series of heteroarylsulfonamide ligands, and their "benzo-extended" analogs (Scheme 1), to human carbonic anhydrase II (HCA; EC 4.2.1.1). In these binding events, the addition of a benzo group: i) increased the hydrophobic surface area (and the volume) of the ligand; ii) generated two new van der Waals contacts between the ligand and hydrophobic wall of HCA; but iii) did not result in a significant increase in the area of contact between the hydrophobic surfaces of the protein and ligand. The free energy of binding of the arylsulfonamide ligands increased with the additional surface area buried upon binding from the benzo-extension by -20 cal mol^{-1}Å^{-2},[3] an amount expected for normal hydrophobic effects (-20 to -33 cal mol^{-1}Å^{-2})[4]. The heat capacity of binding ($\Delta C_\mathrm{p}^\mathrm{o}$) of the benzo-extended ligands was more negative than the corresponding
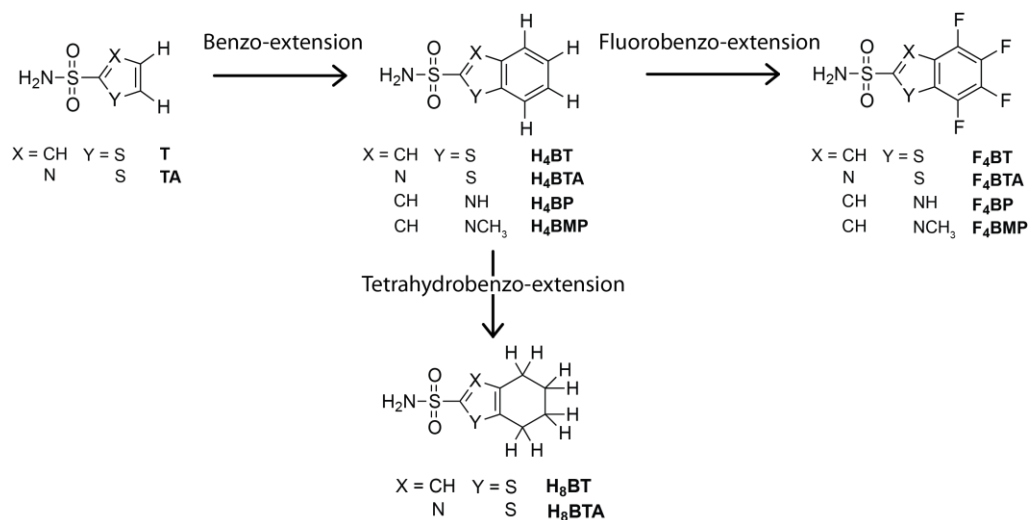
Scheme 1. Arylsulfonamide ligands. Hydrophobic surface area is added to the heterocyclic ligands by: a "benzo-extension", denoted with a **H₄**; a "fluorobenzo-extension", denoted with a **F₄**; or a "tetrahydrobenzo-extension", denoted with a **H₈**. The bold letters are the ligand acronyms: (**B**)**TA** = (benzo)thiazole; (**B**)**T** = (benzo)thiophene; (**B**)**P** = (benzo)pyrrole; (**B**)**MP** = *N*-methyl(benzo)pyrrole.

arylsulfonamide[3]—a change commonly considered to be a sign of a hydrophobic interaction.[5]

We drew two conclusions pertinent to protein-ligand interactions from the previous study:[3] i) the balance of enthalpy and entropy responsible for the differences in the partitioning of a ligand, and its benzo-extended analog, between octanol and buffer is not the same as that responsible for differences in the binding of these ligands to HCA; and ii) the increased binding affinity of the benzo-extended ligands to HCA results from an increased favorability in the enthalpy of binding, and not from an increased entropy of binding. The enthalpy-driven binding observed between these ligands and HCA is not compatible with the mechanism of the hydrophobic effect proposed by Kauzmann and Tanford (KT),[4, 6] but is similar to those observed in other protein-ligand systems.[7-9] We—along with Berne,[10] Chandler,[11] Friesner,[12, 13] Klebe,[14] Ladbury,[15, 16] Lemieux,[17] Rossky,[18, 19] and Toone[20, 21]—attribute this type of enthalpy-dominated hydrophobic effect to the release of water from the binding pocket upon binding of the ligand. Similar thermodynamic signatures characterize binding of the benzo and the tetrahydrobenzo derivative of **T** (see Scheme 1).[3]

The objective of this work was to determine if replacing the four $C-H$ bonds of the benzo moiety with four $C-F$ bonds (i.e., "fluorobenzo-extension") would change the hydrophobic interactions of these ligands with HCA. Fluorocarbons are commonly believed to be "more hydrophobic" than homologous hydrocarbons,[22, 23] but typical measures of hydrophobicity— when corrected for differences in surface area—are very similar, if not indistinguishable.[9, 23, 24] We measured the partitioning of the benzo- and fluorobenzo-extended ligands between buffer and octanol, and found the surface area-corrected hydrophobicity of the ligands increases (by ~ 1.1 cal mol^{-1} Å^{-2}) upon fluorination (summarized in the Supporting Information (SI)).

Benzo- and fluorobenzo-extended ligands bind to HCA with similar geometry. Crystal structures of HCA complexed with **F₄BTA**, **H₄BTA**, and **H₈BTA** (Figure 1) show that the geometry of binding of these ligands is similar in orientation despite their differences in shape, volume, and surface. The geometries of binding of **F₄BT**, **H₄BT**, and **H₈BT** are also conserved (see SI).

Careful inspection of the crystal structures of **H₄BTA** and **F₄BTA** reveals that fluorination of the ligand shifts its position within the binding pocket by 0.7 Å (Figure 1D) while the positions of the side chains of the amino acids lining the binding pocket of HCA do not change. We attribute this shift of **F₄BTA** to an increased number of unfavorable interactions between the ligand and the binding pocket (Figure 1E); in particular, the Coulombic repulsion between the fluorine atom on the ligand and the carbonyl of Thr 200,[25] a 3.0 Å distance.

The atomic composition of the benzo-extension does not affect binding affinity. We measured the enthalpies of binding ($\Delta H^{\mathrm{o}}_{\mathrm{bind}}$) and the association constants (K_{a}) for the series of ligands in Scheme 1 using isothermal titration calorimetry (ITC), and estimated the free energies ($\Delta G^{\mathrm{o}}_{\mathrm{bind}}$) and entropies ($-\mathrm{T}\Delta S^{\mathrm{o}}_{\mathrm{bind}}$) of binding. To account for differences in the pK_{a} of each ligand, we corrected the measured thermodynamic parameters to represent the binding of the sulfonamide anion to HCA (details in the SI).[26]

Remarkably, values of $\Delta G^{\mathrm{o}}_{\mathrm{bind}}$ of the benzo- and fluorobenzo-extended compounds are indistinguishable at a 90% confidence level (Figure 2A). Values of $\Delta G^{\mathrm{o}}_{\mathrm{bind}}$, combined with the overall conserved binding geometry of each set of benzo- and fluorobenzo-extended ligands
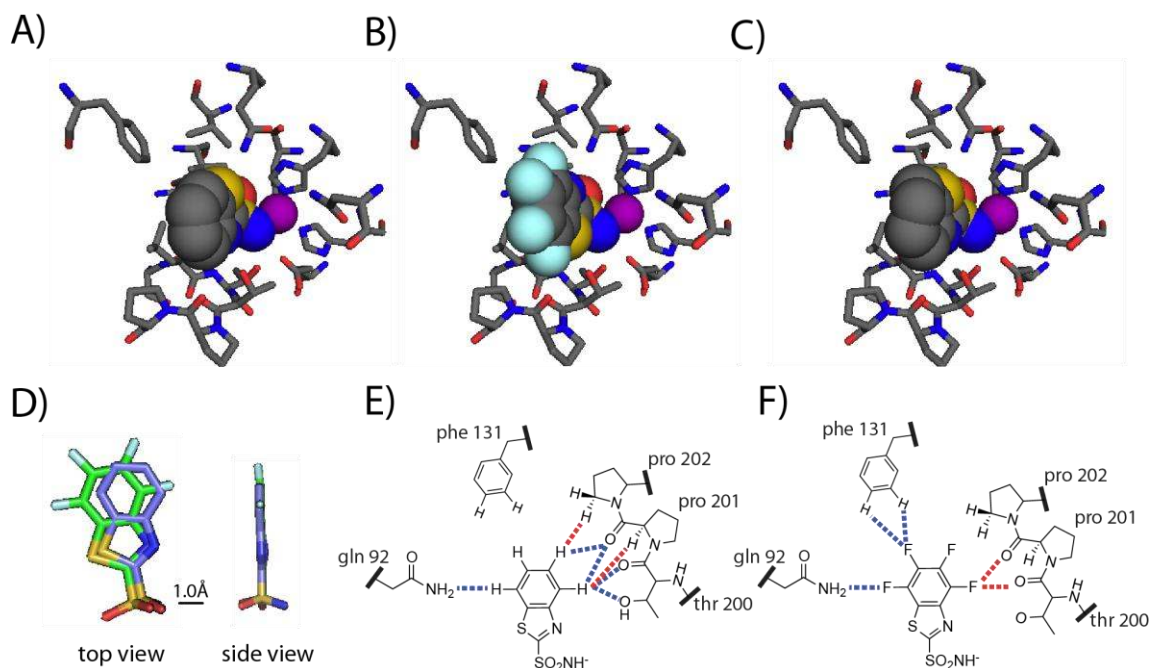
Figure 1. Crystal structures of the active site of HCA complexed with A) **H₄BTA**, B) **F₄BTA**, and C) **H₈BTA**. The Zn^{+2} ion is represented by a purple sphere in each structure. D) An overlay of the heavy atoms of the **H₄BTA** (blue) and **F₄BTA** (green) ligands from aligned crystal structures. Diagrams of the amino acid residues in contact with the E) benzo-extended portion of **H₄BTA**, and F) the fluorobenzo-extended portion of **F₄BTA**. Favorable interactions between the ligand and the protein are represented with a blue dashed line, and unfavorable interactions with a red dashed line.

suggests that binding depends on a fine balance of interactions between HCA, the ligand, and molecules of water filling the pocket and surrounding the ligand, and that a simple analysis of interactions between the protein and ligand (Figure 1E), or of the physiochemical properties of the ligands, is insufficient to understand (or more importantly, predict) the energetics of binding. Our previous study of H_4BT and H_8BT showed that changes in the shape of the ligand also resulted in indistinguishable values of ΔG^{o}_{bind}.[3]

The increased binding affinity of **TA** (or **T**) upon benzo- and fluorobenzo-extension is an enthalpy-dominated hydrophobic interaction, and not the "classical hydrophobic" effect described by KT. We showed previously that the interactions between the benzo-extended ligands and HCA do not result from a "non-classical hydrophobic effect",[27] because the binding of H_8BT is also enthalpy-dominated.[3] The partitioning of H_4BTA and F_4BTA from buffer into octanol (Figure 2B) is, however, an entropy-dominated hydrophobic effect, and in agreement with the KT model.

The release of water from the binding pocket, and not contact between the protein and ligand, affects binding affinity. Comparisons of the crystal structures of H_4BMP and H_4BTA (or F_4BMP and F_4BTA, Figure 3) show that the positions of the side chains of the amino acids lining the binding pocket of HCA do not change, even when the geometry of the bound ligand shifts significantly. The root-mean square deviation for the heavy atoms of the protein in the aligned structures is 0.185 Å for H_4BMP and H_4BTA, 0.214 Å for F_4BMP and F_4BTA, and (for comparison) 0.200 Å for H_4BTA and F_4BTA.

The values of ΔG^{o}_{bind} for H_4BMP and F_4BMP are also indistinguishable ($\Delta\Delta G^{o}_{bind} = 0.7 \pm 0.1$ kcal mol^{-1}), and enthalpy-dominated. These results support our hypothesis that the increased binding affinity of the benzo-extended ligands is independent of the change in atomic
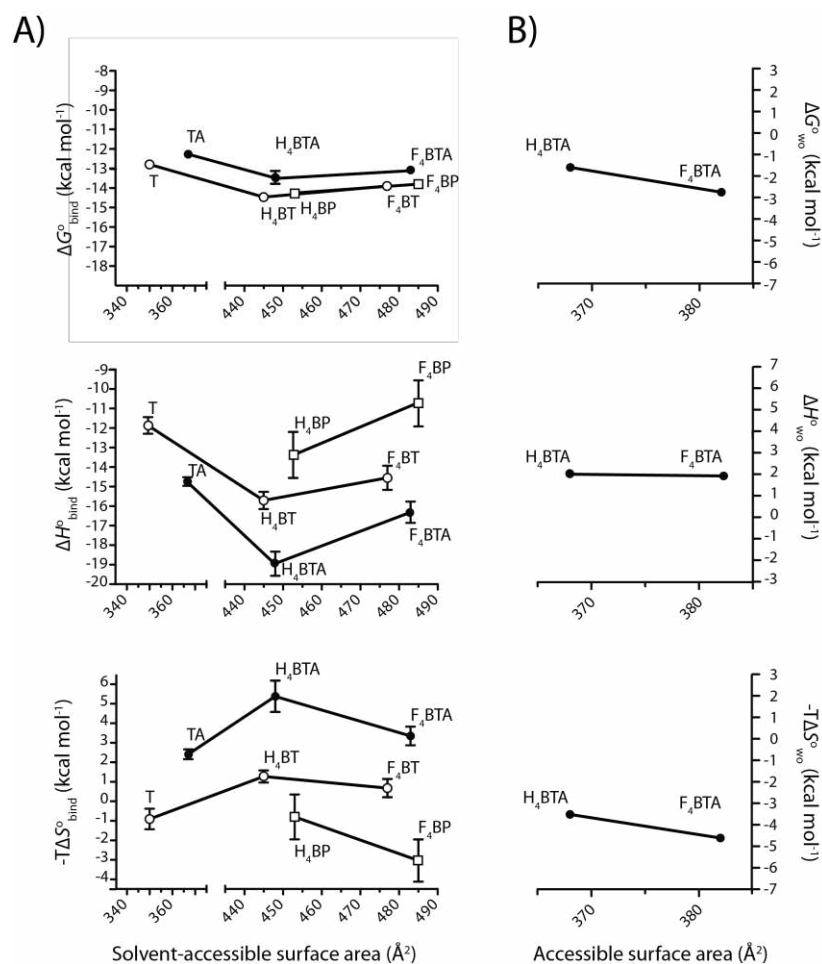
Figure 2. A) Thermodynamics of binding of the anion of each arylsulfonamide ligand to HCA as a function of the difference in solvent-accessible surface area between the bound and unbound states of the ligand. Each datum is the average of at least seven independent measurements, and the error bars represent one standard deviation from the mean (many of the error bars for the values of ΔG^{o}_{bind} are too small to distinguish). B) Thermodynamics of partitioning of **H₄BTA** and **F₄BTA** from buffer to octanol; each datum is the average of three independent measurements. The equilibrium constants for partitioning from octanol to buffer of each sulfonamide were measured by a shake-flask method. Values for the enthalpy of partitioning of each ligand represent the difference between the enthalpy of dissolution into buffer and the

enthalpy of dissolution into octanol. Values for the thermodynamics of partitioning and binding

are corrected for the ionization of the sulfonamide group in the buffer phase.[3]

composition of the benzo group, and almost indistinguishable for three types of functional groups that have very different molecular properties.

While the $\Delta G^{\text{o}}_{\text{bind}}$ is unchanged upon fluorination, we observe significant and compensating changes in $\Delta H^{\text{o}}_{\text{bind}}$ and $-\text{T}\Delta S^{\text{o}}_{\text{bind}}$ (Figure 2A). To elucidate potential sources for the differences in the $\Delta H^{\text{o}}_{\text{bind}}$ and $-\text{T}\Delta S^{\text{o}}_{\text{bind}}$ we calculated the molecular mechanics implicit solvent binding energy (with Prime MM-GBSA calculations[28]) of **H$_4$BTA** and **F$_4$BTA**, and decomposed these values into individual energetic components (i.e., Coulombic, van der Waals, desolvation, ligand strain, etc.). The differences between the individual components of the binding energy of **H$_4$BTA** and **F$_4$BTA** are similar (less than 1.5 kcal mol^{-1} different, see SI) except for: the Coulombic term, which favors the binding of **H$_4$BTA** by 5.8 kcal mol^{-1}; and the desolvation term, which favors the binding of **F$_4$BTA** by 8.2 kcal mol^{-1}.

The crystal structures of **H$_4$BTA** and **F$_4$BTA** (Figure 1E) support the improved Coulombic interactions between **H$_4$BTA** and the binding pocket of HCA; this picture is further supported by the more favorable $\Delta H^{\text{o}}_{\text{bind}}$ of **H$_4$BTA** over **F$_4$BTA**. The desolvation of **F$_4$BTA** is more favorable than **H$_4$BTA**, and is consistent with the values of $-\text{T}\Delta S^{\text{o}}_{\text{bind}}$ (Figure 2A) and free energy and entropy of partitioning (Figure 2B) of both ligands. The free energy of desolvation of the ligand is a primary contributor, along with conformational energy, to the $-\text{T}\Delta S^{\text{o}}_{\text{bind}}$ associated with protein-ligand binding.[29] We assume the role of the conformational entropy in the HCA-ligand complexes is minimal because of the rigidity of the binding pocket of HCA and the conserved binding geometry of each ligand; this rigidity stems from the fact that there is only a single, rotatable bond (the Ar-SO$_2$NH$^-$ bond) in the molecule.

The Prime MM-GBSA calculations predict a more favorable total free energy of binding of HCA with **F$_4$BTA** over **H$_4$BTA** (by < 3.0 kcal mol^{-1}). The zero-temperature model used in MM-

GBSA calculations, however, tend to overestimate the predicted magnitude of ΔG^{o}_{bind} (by ~3-fold[30]). The adjusted value of ΔG^{o}_{bind} for the MM-GBSA calculations is within the experimental error of our ITC measurements, and agrees (qualitatively) with the indistinguishable values of ΔG^{o}_{bind} we measured for **H₄BTA** and **F₄BTA**.

Different benzo-extensions cause similar effects on the water molecules inside the protein pocket upon binding. Crystal structures of HCA complexed with **H₄BTA** or **F₄BTA** show that fluorination of the benzo-extended ligands increases the number of localized (i.e., crystallographically resolvable) waters in the binding pocket of HCA from six to ten. We summarize the number of fixed molecules of water for the benzo- and fluorobenzo-extended **BTA** and **BMP** ligands in Table 1. This result mirrors our previous study,[3] which showed that the addition of the benzo-extension to the arylsulfonamide ligands increased the number of fixed waters within the binding pocket of HCA. The number of waters localized by the benzo-extended ligands cannot be attributed solely to the surface area of the ligand—**H₄BTA** = 448 Å^2, **F₄BTA** = 483 Å^2—because **H₈BTA** (470 Å^2) has a larger surface area than **H₄BTA**, but localizes a smaller number of waters (SI).

We measured values of ΔH^{o}_{bind} of **TA**, **H₄BTA**, and **F₄BTA** over a temperature range of 288 − 307 K, plotted ΔH^{o}_{bind} as a function of temperature, and applied a linear fit to each set of data to determine the heat capacity of binding (ΔC^{o}_{p}) for each ligand: **TA** = −13 cal mol^{-1} K^{-1}, **H₄BTA** = −64 cal mol^{-1} K^{-1}, and **F₄BTA** = −108 cal mol^{-1} K^{-1}. The ΔC^{o}_{p} of each ligand is negative, and is compatible with our hypothesis that the interaction between the ligand and the protein is hydrophobic in nature.[5]

The difference in the heat capacity of **F₄BTA** and **H₄BTA** ($\Delta\Delta C^{o}_{p} = \Delta C^{o}_{p}$(**F₄BTA**) − ΔC^{o}_{p} (**H₄BTA**) = −44 cal mol^{-1} K^{-1}) is much larger than the difference calculated from the buried,
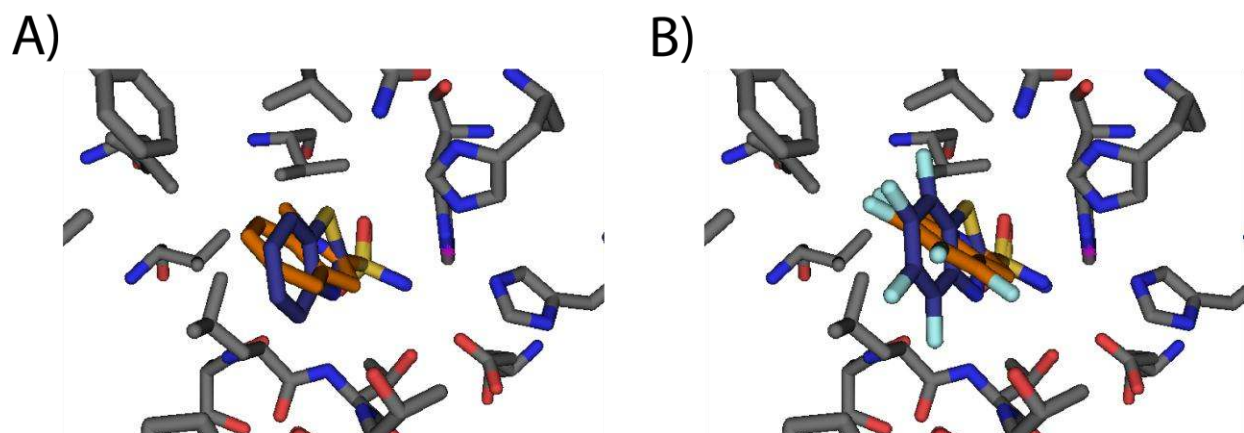
Figure 3. Side-by-side comparison the active site of HCA complexed with **(F)BTA** (blue) and **(F)BMP** (orange). A) **H₄BTA** and **H₄BMP** and B) **F₄BTA** and **F₄BMP**.

non-polar surface area of the two ligands (-19 cal mol^{-1} K^{-1}).[5] We attribute this discrepancy between the measured and predicted values of ΔC°_{p} to the additional "fixed" waters observed in the crystal of **F$_4$BTA** bound to HCA (Figure 1D). The value estimated by Connelly for the ordering of a single water (-9 cal mol^{-1} K^{-1})[31] suggests that three additional molecules of water are fixed in the binding pocket of HCA when the hydrogen atoms of **H$_4$BTA** are replaced with fluorine atoms, and is consistent with the four additional waters observed in the crystal structure.

Increases in binding affinity of ligands correlates with the number of waters released from the binding pocket of HCA, and not with the atomic composition or structure of the ligand. The calorimetry and X-ray crystallography data for the binding of benzo- and fluorobenzo-extended arylsulfonamide ligands to HCA reinforce our previous conclusion:[3] the hydrophobic effect involved in the binding of arylsulfonamide ligands to HCA is *not* dominated by a direct interaction between the hydrophobic surfaces of the protein and the ligand, but is a result of a more general interaction in which the non-polar ligand displaces free-energetically unfavorable waters from the binding pocket into the bulk.

The ΔG°_{bind} of these ligands is independent of both the orientation of the ligand in the binding pocket of HCA, and the atoms in the benzo-extension as both ligands displace a similar number of water molecules from the binding pocket. The addition of a benzo-extension to the heterocyclic sulfonamide ligand results in a favorable increase in ΔH°_{bind}; the model proposed by KT does not explain the binding of these ligands to HCA, but is compatible with their partitioning between buffer and octanol. Replacing the four hydrogen atoms of the benzo-extension with fluorine atoms does result, however, in a decreased favorability of ΔH°_{bind} and an increased favorability of $-\mathrm{T}\Delta S^{\circ}_{bind}$. The compensation of ΔH°_{bind} and $-\mathrm{T}\Delta S^{\circ}_{bind}$ can be

rationalized in terms of the Coulombic interactions of each ligand with the binding pocket of HCA (i.e., the $\Delta H^{\mathrm{o}}_{\mathrm{bind}}$ term) and the changes in the energy of solvation (i.e., the $-\mathrm{T}\Delta S^{\mathrm{o}}_{\mathrm{bind}}$ term) of the benzo-extended ligand upon fluorination.

These differences in the thermodynamics of partitioning of these ligands from buffer to octanol, and from buffer to the binding pocket of HCA, support the idea that there is not a single hydrophobic effect reflecting release of water from contacting surfaces of HCA and ligand, but rather aggregated hydrophobic *effects* that are dependent on the structure of water in the binding pocket of HCA, and on the structure of water surrounding the ligand.

Supporting Information for this article is available on the WWW under http://dx.doi.org/10.1002/anie.XXXXXXXX.

Table 1. Summary of thermodynamic and structural data for the thiazole and methyl-pyrrole ligands

Ligand	**H$_4$BTA**	**F$_4$BTA**	**H$_4$BMP**	**F$_4$BMP**
$\Delta G^{\mathrm{o}}_{\mathrm{bind}}$ [kcal mol^{-1}]	−13. 5 ± 0.4	−13.0 ± 0.2	−13.2 ± 0.1	−13.3 ± 0.1
$\Delta\Delta G$	| --- Indistinguishable --- |		| --- Indistinguishable --- |	
$\Delta H^{\mathrm{o}}_{\mathrm{bind}}$ [kcal mol^{-1}]	−18.9 ± 0.5	−16.3 ± 0.6	−12.4 ± 0.5	−8.4 ± 0.6
$-\mathrm{T}\Delta S^{\mathrm{o}}_{\mathrm{bind}}$ [kcal mol^{-1}]	5.5 ± 0.7	3.4 ± 0.5	–0.7 ± 0.5	−4.8 ± 0.7
$\Delta\Delta C^{\mathrm{o}}_{\mathrm{p}}$ [cal mol^{-1}][a]	| --- −44 --- |		Not measured	
Fixed waters[b]	6	10	4	7
ΔGeometry (relative to H$_4$BTA)	---	Translation (0.7 Å)[c]	Rotation (27°)[d]	Rotation (31°)[d]

[a] $\Delta\Delta C^{\mathrm{o}}_{\mathrm{p}} = \Delta C^{\mathrm{o}}_{\mathrm{p}}(\mathbf{F_4BTA}) - \Delta C^{\mathrm{o}}_{\mathrm{p}}(\mathbf{H_4BTA})$

[b] Obtained from crystal structures of HCA-ligand complex.

[c] Ligand moves in the direction of Gln 92.

[d] Rotation along the long axis of the ligand.

References.

[1]   W. Blokzijl, J. B. F. N. Engberts, *Angew. Chem., Int. Ed.* **1993**, *32*, 1545.

[2]   N. T. Southall, K. A. Dill, A. D. J. Haymet, *J. Phys. Chem. B* **2002**, *106*, 521.

[3]   P. W. Snyder, J. Mecinovic, D. T. Moustakas, S. W. Thomas, M. Harder, E. T. Mack, M. R. Lockett, A. Heroux, W. Sherman, G. M. Whitesides, *Proc. Nat. Acad. Sci., U.S.A.* **2011**, *108*, 17889.

[4]   C. Tanford, *Proc. Nat. Acad. Sci., U.S.A.* **1979**, *76*, 4175.

[5]   N. V. Prabhu, K. A. Sharp, *Ann. Rev. Phys. Chem.* **2005**, *56*, 521.

[6]   W. Kauzmann, *Ann. Rev. Phys. Chem.* **1957**, *8*, 413.

[7]   W. P. Jencks, *Catalysis in Chemistry and Enzymology*, McGraw-Hill, New York, New York, **1969**.

[8]   S. W. Homans, *Drug Discov. Today* **2007**, *12*, 534.

[9]   J. Mecinovic, P. W. Snyder, K. A. Mirica, S. Bai, E. T. Mack, R. L. Kwant, D. T. Moustakas, A. Heroux, G. M. Whitesides, *J. Am. Chem. Soc.* **2011**, *133*, 14017.

[10]   B. J. Berne, J. D. Weeks, R. Zhou, *Ann. Rev. Phys. Chem.* **2009**, *60*, 85.

[11]   K. Lum, D. Chandler, J. D. Weeks, *J. Phys. Chem. B* **1999**, *103*, 4570.

[12]   R. Chakrabarti, A. Klibanov, R. Friesner, *Proc. Nat. Acad. Sci., U.S.A.* **2005**, *102*, 10153.

[13]   R. Abel, T. Young, R. Farid, B. Berne, R. Friesner, *J. Am. Chem. Soc.* **2008**, *130*, 2817.

[14]   A. Biela, N. N. Nasief, M. Betz, A. Heine, D. Hangauer, G. Klebe, *Angew. Chem., Int. Ed.* **2013**, *52*, 1.

[15]   T. S. G. Olsson, J. E. Ladbury, W. R. Pitt, *Protein Sci.* **2011**, *20*, 1607.

[16]   T. S. G. Olsson, M. A. Williams, W. R. Pitt, J. E. Ladbury, *J. Mol. Biol.* **2008**, *384*, 1002.

[17]   R. U. Lemieux, *Acc. Chem. Res.* **1996**, *29*, 373.

[18]   N. Giovambattista, C. F. Lopez, P. J. Rossky, P. G. Debenedetti, *Proc. Nat. Acad. Sci., U.S.A.* **2008**, *105*, 2274.

[19]   P. J. Rossky, M. Karplus, *J. Am. Chem. Soc.* **1979**, *101*, 1913.

[20]   M. C. Chervenak, E. J. Toone, *J. Am. Chem. Soc.* **1994**, *116*, 10533.

[21]   T. G. Oas, E. J. Toone, *Adv. Biophys. Chem.* **1997**, *6*, 1.

[22]   J. D. Dunitz, *ChemBioChem* **2004**, *5*, 614.

[23]   M. Salwiczek, E. K. Nyakatura, U. I. M. Gerling, S. Ye, B. Koksch, *Chem. Soc. Rev.* **2012**, *41*, 2135.

[24]   J. C. Biffinger, H. W. Kim, S. G. DiMagno, *ChemBioChem* **2004**, *5*, 622.

[25]   A. Bondi, *J. Phys. Chem.* **1964**, *68*, 441.

[26]   V. M. Krishnamurthy, G. K. Kaufman, A. R. Urbach, I. Gitlin, K. L. Gudiksen, D. B. Weibel, G. M. Whitesides, *Chem. Rev.* **2008**, *108*, 946.

[27]   E. A. Meyer, R. K. Castellano, F. Diederich, *Angew. Chem., Int. Ed.* **2003**, *42*, 1210.

[28]   P. D. Lyne, M. L. Lamb, J. C. Saeh, *J. Med. Chem.* **2006**, *49*, 4805.

[29]   E. Freire, *Drug Discov. Today* **2008**, *13*, 869.

[30]   R. Abel, N. K. Salam, J. Shelley, R. Farid, R. A. Friesner, W. Sherman, *ChemMedChem* **2011**, *6*, 1049.

[31]   P. R. Connelly, *Structure-Based Drug Design: Thermodynamics, Modeling and Strategy*, Springer, Berlin, **1997**.

The Binding of Benzoarylsulfonamide Ligands to Human Carbonic Anhydrase is Insensitive to Formal Fluorination of the Ligands

Heiko Lange,[a,†] Matthew R. Lockett,[a,†] Benjamin Breiten,[a] Annie Heroux,[b] Woody Sherman,[c]

Dmitrij Rappoport,[a] Patricia O. Yau,[a] Philip W. Snyder,[a]

George M. Whitesides[a,d,*]

[a] *Department of Chemistry and Chemical Biology, Harvard University*
12 Oxford Street, Cambridge, MA 02138
[b] *National Synchrotron Light Source, Brookhaven National Laboratory*
725 Brookhaven Avenue, Upton, NY 11973-5000
[c] *Schrödinger Inc.,*
120 West 45th Street, New York, NY 10036-4041
[d] *Wyss Institute for Biologically Inspired Engineering, Harvard University*
60 Oxford Street, Cambridge, MA 02138

Expression and Purification of Human Carbonic Anhydrase

We chose human carbonic anhydrase II (HCA, E.C. 4.2.1.1) as a model protein to study the hydrophobic effect in protein-ligand binding, because HCA: i) is well-characterized structurally,[1] and has a binding pocket comprised of a distinct "hydrophobic wall" and a distinct "hydrophilic wall";[1] ii) is structurally rigid, and retains its secondary and tertiary structure upon binding of a ligand;[1, 2] iii) can be expressed in *E. coli* in the quantities necessary for calorimetry experiments and X-ray crystallography; iv) crystallizes readily, and the conditions for growing crystals, reproducibly, are known.[3]

We expressed HCA in BL21(DE3)pLysS competent cells (Promega, Madison, WI), transformed with a pACA plasmid containing the HCA gene,[4][5] according to the procedures published by Fierke and coworkers.[5] After expression, the cultures of *E. coli* were pelleted (20 min, 10,000 x *g*, 4 °C), flash frozen under liquid nitrogen, and stored at –80 °C until needed.

We lysed the *E. coli* with BPER protein extraction buffer (Thermo Scientific) augmented with: $MgSO_4$ (1 mM), *N-p*-tosyl-L-arginine methyl ester (TAME, 1 mM), tris(2-carboxyethyl)phosphine (TCEP, 3 mM), $ZnSO_4$ (2.5 mM), phenylmethanesulfonyl fluoride (PMSF, 1 μM), lysozyme (0.125 μg / mL), and DNase I (10 U / mL). The HCA was precipitated from the cellular lysate with ammonium sulfate (60% v/v with a solution of saturated ammonium sulfate), and then dialyzed into Tris-SO_4 buffer (50 mM, pH = 8.0) containing $ZnSO_4$ (200 μM) and TCEP (200 μM). The dialyzed protein was further purified on an AKTA purifier (GE Healthcare) with: i) anion exchange chromatography with Q Sepharose Fast Flow resin (Sigma Aldrich); and ii) size exclusion chromatography with SuperDex 75 resin (GE Healthcare). We used Tris-SO_4 buffer (50 mM, pH = 8.0) containing $ZnSO_4$ (200 μM) and TCEP (200 μM) for all chromatographic separations.

Synthesis of the Heteroarylsulfonamide Ligands

We synthesized the benzo- and fluorobenzo-extended ligands from commercially available starting materials, which we used without further purification (Sigma Aldrich, Alfa Aesar, TCI, and 3B Scientific Corporation). We characterized the final product of each synthesis with ^{1}H and ^{19}F NMR spectroscopy, and GC-MS (EI). We measured ^{1}H and ^{19}F spectra on a 300 or 400 MHz instrument, and report the chemical shifts (in ppm) relative to tetramethylsilane for ^{1}H NMR spectra, and relative to trichloro-fluoromethane for ^{19}F NMR spectra. Coupling constants (*J*) are given in Hz, and the apparent resonance multiplicities are abbreviated with (b)s ((broad) singlet), d (doublet), t (triplet), and m (multiplet). We measured the mass of each compound with an Agilent GC/MSD 5975A inert with a Triple-Axis Detector, controlled *via* Agilent GC ChemStation Software (version E.02.00.493), containing a HP 5MS column (5% diphenyl 95% dimethylpolysiloxane, 30 m x 0.25 mm).

We synthesized the benzo-extended ligands according to previously published synthetic procedures: benzo[*b*]thiophene-2-sulfonamide (**H₄BT**),[6] benzo[*d*]thiazole-2-sulfonamide (**H₄BTA**),[6] 1*H*-indole-2-sulfonamide (**H₄BP**),[7] 1-methyl-1*H*-indole-2-sulfonamide (**H₄MBP**),[8] 4,5,6,7-tetrahydrobenzo[*b*]thiophene-2-sulfonamide (**H₈BT**),[9] and 4,5,6,7-tetrahydrobenzo[*d*]thiazole-2-sulfonamide (**H₈BTA**).[10] We stored all ligands under argon or nitrogen at room temperature.

General Synthetic Procedure for Fluorobenzo-extended Ligands. If not stated otherwise, the fluorobenzo-extended ligands were synthesized following a general synthetic procedure (**GP**) developed by Chern *et al.*[6] The starting material (typically 10 mmol, 1 equiv.) was dissolved in dry tetrahydrofuran (THF) under an argon atmosphere, cooled to −78° C, and reacted with a 1.6 M solution of *n*-butyllithium in hexanes (1.1 equiv.). The reaction mixture was stirred for 1 hour,

and allowed to warm to ca. 0° C before the intermediate aryl lithium species was quenched with dry gaseous sulfur dioxide. Sulfur dioxide was blown over the surface of the reaction solution for approximately five minutes to exchange the atmosphere in the flask, and the flask re-sealed with a balloon filled with gaseous sulfur dioxide. The reaction mixture was stirred for an additional hour, and the reaction mixture was allowed to warm to room temperature. Argon was then bubbled through the reaction suspension to remove the excess of sulfur dioxide, and the resulting slurry was concentrated *in vacuo* to yield the lithium benzoaryl-2-sulfinate as a pasty solid.

The crude lithium sulfinates were re-dissolved in aqueous sodium acetate, hydroxylamine-*O*-sulfonic acid (2.5 equiv.) was added at 0° C, and the mixture stirred overnight at room temperature. The precipitate was isolated by filtration, washed with cold water, and the fluorobenzo-extended ligands recrystallized.

4,5,6,7-tetrafluorobenzo[b]thiophene-2-sulfonamide (F₄BT). **F₄BT** was synthesized, according to the general procedure (**GP**) outlined above, from 4,5,6,7-tetrafluorobenzo[*b*]thiophene, which was prepared from 4,5,6,7-tetrafluorobenzo[*b*]thiophen-2-carboxylic acid[11] using a copper-catalyzed decarboxylation described previously.[12]

^{1}H NMR (300 MHz, DMSO-d_6) δ 8.17 (bs, 2H), 7.54 (s, 1H); ^{19}F NMR (282 MHz, DMSO-d_6) δ −137.5 (dd, J = 14.4, 21.4), −147.0 (dd, J = 14.8, 20.8), −155.7 (t, J = 21.3), −156.4 (t, J = 20.8); GC-MS (EI, 70 eV): m/z 284.9 (M$^+$, 100%) @ t_R 21.8 min.

4,5,6,7-tetrafluorobenzo[d]thiazole-2-sulfonamide (F₄BTA). **F₄BTA** was prepared from 2,3,4,5,6-pentafluoroaniline, which was prepared from 4,5,6,7-tetrafluorobenzo[*d*]thiazole-2-thione.[13] The thione was reacted with an aqueous solution of ammonia in the presence of sodium hydroxide and sodium hypochlorite to yield the intermediate *S*-

(perfluorobenzo[d]thiazol-2-yl)thiohydroxylamine.[14] The latter was isolated and treated with hydrogen peroxide solution to furnish **F₄BTA** after re-crystallization.

^{1}H NMR (300 MHz, DMSO-d_6) δ 8.68 (bs, 2H); ^{19}F NMR (282 MHz, DMSO-d_6) δ −137.5 (dd, J = 14.4, 21.4), −147.0 (dd, J = 14.8, 20.8), −155.7 (t, J = 21.3), −156.4 (t, J = 20.8); GC-MS (EI, 70 eV): m/z 268.9 ([M − H$_2$O]$^+$, 100%) @ t_R 13.0 min.

4,5,6,7-tetrafluorobenzo[b]-1H-pyrrole-2-sulfonamide (F₄BP). **F₄BP** was synthesized from 4,5,6,7-tetrafluoro-1H-indole according to the **GP** outlined above, after the indole-nitrogen was protected with a benzoyl group according to standard protocols.[6] The final product was deprotected according to standard protocols.[6]

^{1}H NMR (300 MHz, DMSO-d_6) δ 7.81 (bs, 2H), 7.10 (s, 1H), 3.35 (bs, ca.1H); ^{19}F NMR (282 MHz, DMSO-d_6) δ −149.4 (dd, J = 17.2, 21.0), −157.6 (dd, J = 17.1, 20.3), −163.5 (t, J = 20.4), −169.0 (dt, J = 21.0, 3.4); GC-MS (EI, 70 eV): m/z 268.0 (M$^+$, 100%) @ t_R 21.2 min.

4,5,6,7-tetrafluorobenzo[b]-N-methyl-pyrrole-2-sulfonamide (F₄MBP). **F₄MBP** was synthesized from 4,5,6,7-tetrafluoro-N-methyl-indole, according to the **GP** outlined above, which was obtained by the methylation of 4,5,6,7-tetrafluoro-1H-indole with methyl iodide in the presence of sodium hydride in dry THF.[6]

^{1}H NMR (300 MHz, DMSO-d_6) δ 8.14 (bs, 2H), 7.10 (s, 1H), 3.31 (s, 3H); ^{19}F NMR (282 MHz, DMSO-d_6) δ −149.6 (dd, J = 16.8, 20.9), −161.9 (t(dd), J = 20.8), −162.9 (t, J = 20.7), −169.0 (dt, J = 21.1, 3.8); GC-MS (EI, 70 eV): m/z 282.0 (M$^+$, 100%) @ t_R 20.3 min.

Physiochemical Characterization of the Heteroarylsulfonamide Ligands

We summarize the physico-chemical data collected for each sulfonamide ligand in Table S1, and discuss the procedures in detail below.

Determination of pKₐ. The pK_a of **T, TA**, **H₄BT**, **H₈BT**, and **H₄BTA** (Figure S1) were determined previously.[2] We used the same procedure to determine the pK_a of the fluorobenzo-extended ligands: a solution of the ligand (20 mM in DMSO) was added to a buffered solution (10 mM, ranging from pH 1 to pH 13 in 0.5 increments of pH) in a cuvette, and a UV-VIS spectrum obtained.

Determination of ΔH^o_{ion}. We could not measure the ΔH^o_{ion} of the fluorobenzo-extended ligands directly with calorimetry due to their low solubility. To approximate values of ΔH^o_{ion}, we correlated the chemical shift of the proton in the sulfonamide group, measured with ^{1}H NMR spectroscopy, with the chemical shift of the proton in the sulfonamide group of known heteroarylsulfonamide ligands (Figure S1) – namely thiophene-2-sulfonamide (**T**), benzothiophene-2-sulfonamide (**H₄BT**), thiazole-2-sulfonamide (**TA**), benzothiazole-2-sulfonamide (**H₄BTA**), furane-2-sulfonamide (**F**), benzofurane-2-sulfonamide (**H₄BF**), imidazole-2-sulfonamide (**I**), benzoimidazole-2-sulfonamide (**H₄BI**), benzopyrrole-2-sulfonamide (**H₄BP**).

Partitioning experiments. We measured the equilibrium constant of partitioning, between sodium phosphate buffer (10 mM, pH = 7.6) and octanol, for each of the benzo- and fluorobenzo-extended ligands using the shake-flask method described previously.[2]

Solution calorimetry. We followed the procedure reported previously,[2] and measured the heat of dissolution for solid samples of each ligand (5–10 mg) with a TAMIII calorimeter (TA Instruments).

Table S1. Physico-chemical properties of the heteroarylsulfonamide ligands, and the Zn(II)-bound-water form of HCA II (HCA-Zn(II)-OH$_2^+$), used in this study.

system ligand	SASA [Å^2]	pK_a	ΔH°_{ion} [kcal mol^{-1}] [a]	log$P$ [b]	ΔG°_{OW} [kcal mol^{-1}]	ΔG°_{OW} per Å^2 [cal mol^{-1} Å^{-2}]
thiophene						
T	301	9.6	8.4	1.62	0.8 ± 0.04	2.7
H$_4$BT	369	9.5	8.1	0.76	1.6 ± 0.1	4.3
F$_4$BT	380	8.6	7.8	−0.44	2.0 ± 0.3	5.3
H$_8$BT	394	9.8 [c]	8.5	n.d.	n.d.	n.d.
thiazole						
TA	296	8.4	7.7	1.46	−0.8 ± 0.03	−2.7
H$_4$BTA	364	8.2	7.4	−0.25	1.3 ± 0.3	3.6
F$_4$BTA	379	7.9	7.2	−1.33	2.5 ± 0.1	6.6
H$_8$BTA	391	n.d.	n.d.	n.d.	n.d.	n.d.
pyrrole						
H$_4$BP	366	9.8	8.5	1.12	1.5 ± 0.2	4.1
F$_4$BP	377	9.4	8.2	0.11	2.3 ± 0.1	6.1
N-methyl pyrrole						
H$_4$MBP	384	9.4	8.2	0.65	1.6 ± 0.3	4.1
F$_4$MBP	402	8.8	7.8	-0.12	1.8 ± 0.6	4.5
protein						
HCA-Zn(II)-OH$_2^{+}$ [d]	n.d.	6.9 (6.9)	6.9	---	---	---

a) NMR experiments were performed in DMSO-d_6 at 25° C.
b) Calculated *via* log$P$ = log$D$ + log(1 + 10$^{pKa\text{-}pH}$).
c) Determined previously by Snyder *et al.*[2]
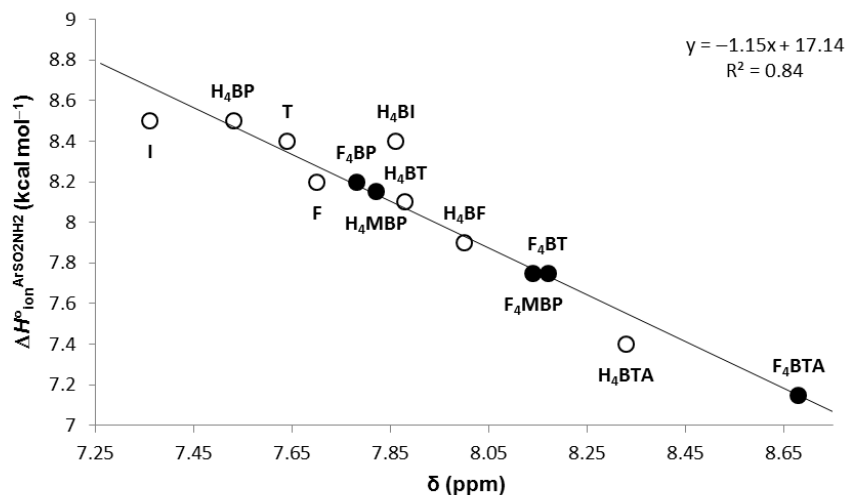d) Values estimated according to the literature.[1]

Figure S1. NMR-based approximation of values of ΔH°_{ion} for the fluorobenzo-extended ligands. The solid black circles represent an independently measured value of ΔH°_{ion} for the fluorobenzo-extended ligands. The hollow circles represent an independently measured value of ΔH°_{ion} from compounds for which ΔH°_{ion} had been independently determined, and reported[2]: **I** – imidazole-2-sulfonamide, **H₄BP** – benzo[*b*]pyrrole-2-sulfonamide, **T** – thiophene-2-sulfonamide, **F** – furane-2-sulfonamide, **H₄BT** – benzo[*b*]thiophene-2-sulfonamide, **H₄BF** – benzo[*b*]furane-2-sulfonamide, **H₄BTA** – benzo[*d*]thiazole-2-sulfonamide We correlated the chemical shift of the sulfonamide proton to obtain the linear curves displayed.

Isothermal Titration Calorimetry

We conducted all ITC experiments on an Auto VP-ITC instrument (Microcal). In each titration experiment, 19 injections of ligand (7.8 μL, 100 μM) were introduced into the calorimeter cell, which contained HCA (1.6 mL, 100 μM), and the heat of binding (ΔH°_{bind}) was recorded. We used sodium phosphate buffer (10 mM, pH = 7.60) for all experiments.

The raw data were analyzed using the Origin software package, and the free energy of binding (ΔG°_{bind}) and entropy of binding ($-T\Delta S^{\circ}_{bind}$) estimated with a nonlinear, single-binding site model. Values of K_a, ΔG°_{bind}, ΔH°_{bind}, and $-T\Delta S^{\circ}_{bind}$ are the average of at least seven experiments and the uncertainties are one standard deviation from the mean.

pK$_a$-correction of observed ITC data: We corrected the K_a of each arylsulfonamide ligand—to reflect the binding of the arylsulfonamide anion ($ArSO_2NH^-$) to the zinc-bound water form of HCA ($HCA\text{-}Zn^{II}\text{-}OH_2^+$)—using a previously reported method,[15] which is explained in detail by Snyder *et al.*[2] Table S2 lists the observed, and the pK$_a$-corrected values of ΔG°_{bind}, ΔH°_{bind}, and $-T\Delta S^{\circ}_{bind}$ for the sulfonamide ligands investigated in this study. Figure S2 shows ΔG°_{bind}, ΔH°_{bind}, and $-T\Delta S^{\circ}_{bind}$ as function of SASA for each ligand.

Table S2. Observed and pK_a-corrected thermodynamic parameters for free energy of binding ($\Delta G°_{bind}$), enthalpy of binding ($\Delta H°_{bind}$), and entropy of binding ($-T\Delta S°_{bind}$) for the anion of each heteroarylsulfonamide ligand to HCA II.

Ligand	N^a	SASA (Å^2)	$\Delta G°_{bind}$ (kcal mol^{-1})		$\Delta H°_{bind}$ (kcal mol^{-1})		$-T\Delta S°_{bind}$ (kcal mol^{-1})	
			observed	corrected[b]	observed	corrected[b]	observed	corrected[b]
thiophene								
T	6	303	−9.0±0.1	−12.8±0.1	−9.4±0.4	−11.9±0.4	0.4±0.5	−0.9±0.5
H₄BT	9	369	−11.2±0.2	−14.4±0.2	−13.7±0.4	−15.7±0.4	2.5±0.3	1.3±0.3
F₄BT	9	380	−11.3±0.2	−13.9±0.2	−13.2±0.6	−14.5±0.6	1.9±0.5	0.7±0.5
H₈BT	7	394	−10.5±0.1	−14.7±0.1	−11.6±0.1	−14.4±0.1	1.1±0.02	0.3±0.1
thiazole								
TA	7	296	−10.0±0.1	−12.3±0.1	−13.9±0.2	−14.7±0.2	−3.8±0.3	−2.5±0.3
H₄BTA	9	364	−11.4±0.3	−13.5±0.3	−18.6±0.6	−18.8±0.6	−7.1±0.8	−5.3±0.8
F₄BTA	9	379	−11.3±0.2	−13.0±0.2	−17.3±0.6	−16.3±0.6	−6.0±0.5	−3.4±0.5
H₈BTA	n.d.	391	n.d.	n.d.	n.d.	n.d.	n.d.	n.d.
pyrrole								
BP	12	366	−10.3±0.1	−14.2±0.1	−10.8±1.2	−13.4±1.2	−0.6±1.2	0.9±1.2
F₄BP	13	377	−10.3±0.2	−13.7±0.2	−8.6±1.2	−10.7±1.2	1.8±1.0	3.0±1.0
N-methyl pyrrole								
H₄MBP	9	384	−9.9±0.1	−13.2±0.1	−10.4±0.5	−12.4±0.5	−0.5±0.5	−0.7±0.5
F₄MBP	6	402	−10.6±0.1	−13.3±0.1	−6.9±0.8	−8.5±0.8	3.7±0.8	4.8±0.8

[a] Number of experiments used for analyses.
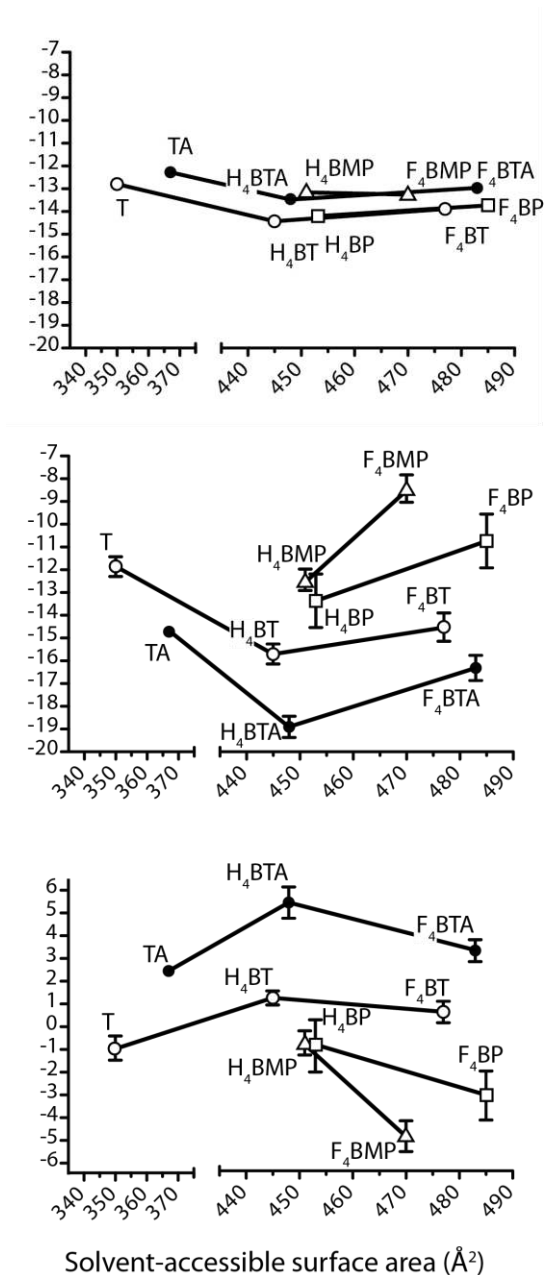[b] Corrected for the pK_a-values determined as described above.

Figure S2. The thermodynamics of binding (i.e., ΔG^o_{bind}, ΔH^o_{bind}, and -TΔS^o_{bind}) of the anions of heteroarylsulfonamide ligands to HCA as a function of the difference in solvent-accessible surface area between the bound and unbound states of the ligand ($\Delta SASA_{unbound} = \Delta SASA_{bound} + \Delta SASA_{protein} - \Delta SASA_{complex}$). Each datum represents the average values of at least seven independent measurements (the error bars represent one standard deviation from the mean).

Decomposition of the Free Energy of Binding Calculations

We calculated the binding energies of **H₄BTA** and **F₄BTA** using the MM-GBSA method[16] (as implemented in Prime[17, 18]). We prepared the initial crystal structure coordinates for the **F₄BTA**-HCA complex with the Protein Preparation Wizard in Maestro (using the **H₄BTA**-HCA complex, PDB code 3S73). The Prime MM-GBSA calculations of each complex held the residues of the binding pocket of HCA rigid and with an energy-minimized structure of the ligand. The binding energy decomposition contained the following terms: Coulombic interactions, van der Waals (vdW) interactions, bonded conformations (bond, angle, and torsion), H-bonding, lipophilic, π-π stacking, and generalized Born solvation. Each component was computed separately for the ligand, the empty binding pocket of HCA, and the ligand-HCA complex and then appropriately summed to calculate each contribution to the total binding energy. The anionic charge on the ligand was computed using a fit to the electrostatic potential derived from quantum mechanics at the RHF/6-31G* level of theory,[19] which has been shown to perform well with continuum solvation models. Energy terms are shown in Table S4.

Biostructural analyses

Protein Crystallization: Monoclinic crystals of HCA were prepared with the hanging drop diffusion method published by McKenna and coworkers,[3] and the crystals of HCA were left undisturbed (at 4 °C) until needed for soaking experiments.

Ligand Soaking Experiments: We soaked the crystals of HCA in saturated solutions of the benzo- and fluorobenzo-extended ligands using the procedure described previously.[2]

Table S4. Decomposition of the Free Energy of Binding for **H₄BTA** and **F₄BTA** (in kcal mol⁻¹).

	Coulomb	vdW	Bonded	H-bond	Lipo	Stacking	Solvation	Total
H₄BTA	−115.2	−26.3	1.2	−0.4	−15.9	0.0	113.5	−43.1
F₄BTA	−109.4	−27.5	1.3	−0.3	−15.4	0.0	105.3	−46.1
Difference	5.8	−1.2	0.1	0.1	0.5	0.0	−8.2	−3.0

X-ray Crystallography: X-ray diffraction data of each crystal was collected at Brookhaven

National Laboratory on the ADSC Quantum Q315 CCD detector at the National Synchrotron

Light Source (beamline X-25) in collaboration with the Mail-Program, Brookhaven National

Laboratory.[20] Reflections were indexed and integrated using HKL2000, and scaled using

SCALEPACK.[21]

Solution of Crystal Structures: Diffraction data were analyzed using the CCP4i suite of

crystallography software[22] using previously published procedures. Table S3 summarizes the

crystallographic details for each protein-ligand structure. Figure S3 shows the images of the

binding pocket of HCA II occupied by the various arylsulfonamide ligands used in this study.

Only protein residues within a 5 Å distance from the ligands are shown. Figure S4 shows
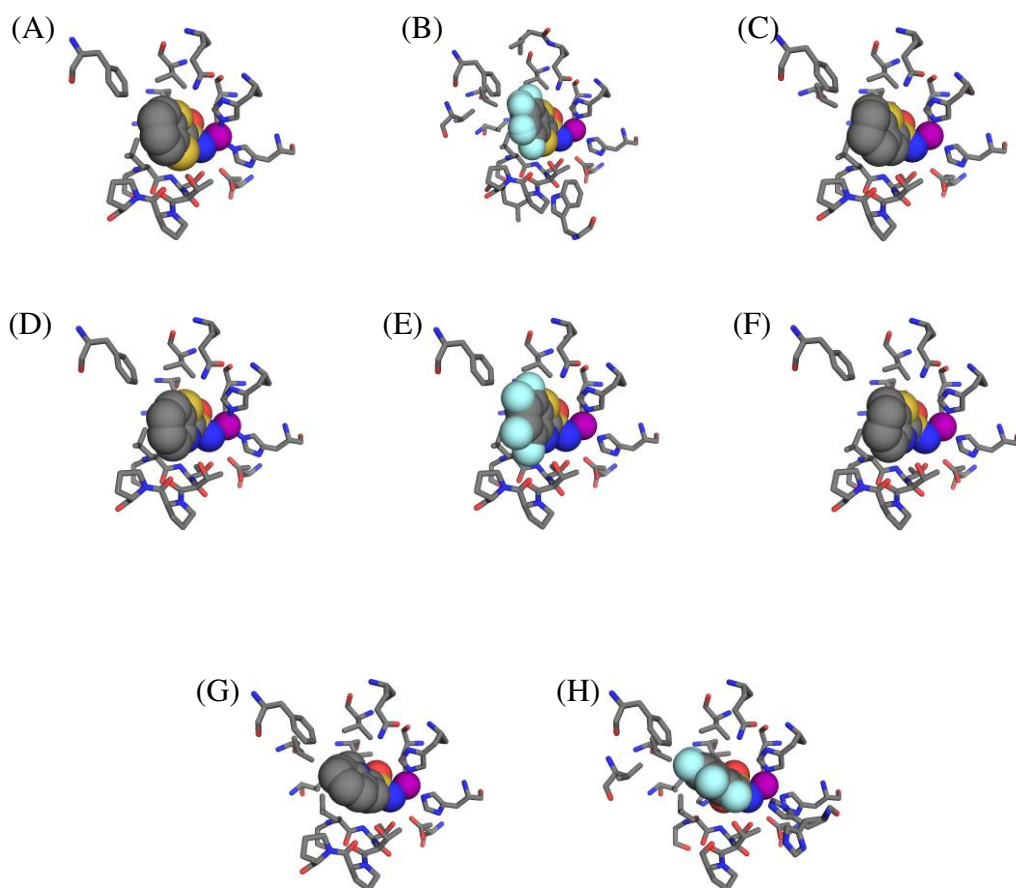
instructive overlays of crystal structures.

Figure S3. Occupied active site of HCA II found in crystal structure analyses of HCA

complexed with: (A) **H₄BT**, (B) **F₄BT,** (C) **H₈BT,** (D) **H₄BTA**, (E) **F₄BTA**, (F) **H₈BTA**, (G)
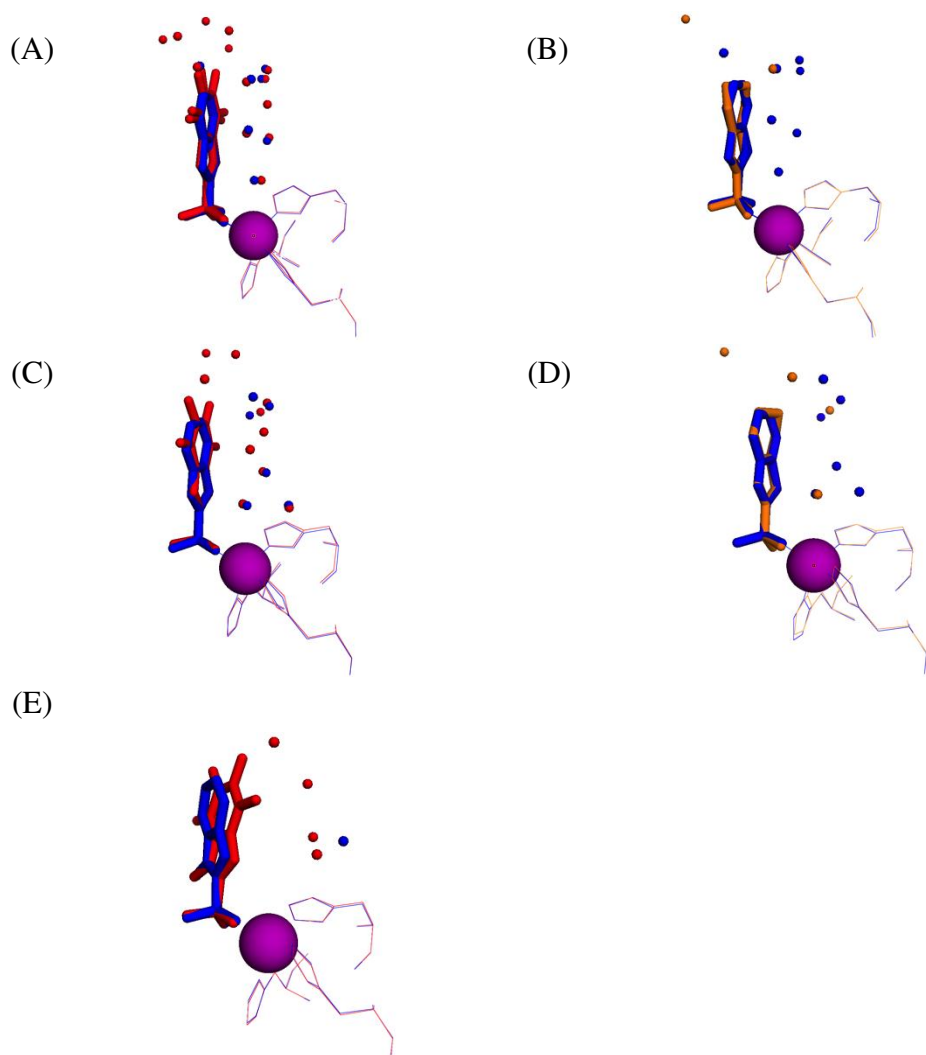
H₄MBP, and (H) **F₄MBP**.

Figure S4. Overlays of benzo-, fluorobenzo-, and tetrahydrobenzo-extended ligands in the active site of HCA. Each overlay contains the crystallographically resolvable waters for: (A) **H$_4$BT** and **F$_4$BT**, (B) **H$_4$BT** and **H$_8$BT**, (C) **H$_4$BTA** and **F$_4$BTA**, (D) **H$_4$BTA** and **H$_8$BTA**, (E) **H$_4$MBP** and **F$_4$MBP**. The benzo-extended ligands are shown in blue, the fluorobenzo-extended ligands in red, and tetrahydrobenzo-extended ligands in orange. In each image, the zinc atom is represented by a purple sphere. We included the three histidine residues that coordinate the zinc atom to show the heavy-atom alignment of proteins in each overlay.

References.

[1]   V. M. Krishnamurthy, G. K. Kaufman, A. R. Urbach, I. Gitlin, K. L. Gudiksen, D. B. Weibel, G. M. Whitesides, *Chem. Rev.* **2008**, *108*, 946.

[2]   P. W. Snyder, J. Mecinovic, D. T. Moustakas, S. W. Thomas, M. Harder, E. T. Mack, M. R. Lockett, A. Heroux, W. Sherman, G. M. Whitesides, *Proc. Nat. Acad. Sci., U.S.A.* **2011**, *108*, 17889.

[3]   A. H. Robbins, J. F. Domsic, M. Agbandje-McKenna, R. McKenna, *Acta Crystallogr., Sect. D: Biol. Crystallogr.* **2010**, *66*, 628.

[4]   The pACA plasmid containing the HCA II gene was a kind gift of the Carol Fierke laboratory (University of Michigan, Department of Chemistry).

[5]   S. K. Nair, T. L. Calderone, D. W. Christianson, C. A. Fierke, *J. Biol. Chem.* **1991**, *266*, 17320.

[6]   J. Chern, Y. Leu, S. Wang, R. Jou, C. Lee, P. Tsou, S. Hsu, Y. Liaw, H. Lin, *J. Med. Chem.* **1997**, *40*, 2276.

[7]   S. L. Graham, J. M. Hoffman, P. Gautheron, S. R. Michelson, R. L. Smith, J. M. Sondey, M. F. Sugrue, *J. Med. Chem.* **1990**, *33*, 749.

[8]   M. Mader, L. Martin-Cabrejas, M. Richett, (Ed.: WIPO), ELI Lilly and Company, **2004**.

[9]   F. Mohamadi, M. Spees, G. Grindey, *J. Med. Chem.* **1992**, *35*, 3012.

[10]   K. Chow, M. Garst, J. Holmes, (Ed.: USPTO), Allergan, **1994**.

[11]   I. M. Shirley, *J. Fluorine Chem.* **1994**, *66*, 51.

[12]   J. G. Pomonis, C. L. Fatland, F. R. Taylor, *J. Chem. Eng. Data* **1976**, *21*, 233.

[13]   L. Zhu, M. B. Zhang, *J. Org. Chem.* **2004**, *69*, 7371.

[14]   C. Proenca, M. L. Serralheiro, M. E. Araujo, T. Pamplona, S. Santos, M. S. Santos, F. Frazao, *J. Heterocycl. Chem.* **2011**, *48*, 1287.

[15]   V. M. Krishnamurthy, B. R. Bohall, C. Y. Kim, D. T. Moustakas, D. W. Christianson, G. M. Whitesides, *Chem. Asian J.* **2007**, *2*, 94.

[16]   I. Massova, P. A. Kollman, *Perspect. Drug Discovery Des.* **2000**, *18*, 113.

[17]   M. P. Jacobson, D. L. Pincus, C. S. Rapp, T. J. F. Day, B. Honig, D. E. Shaw, R. A. Friesner, *Proteins: Struct., Funct., Bioinf.* **2004**, *55*, 351.

[18]   M. P. Jacobson, R. A. Friesner, Z. Xiang, B. Honig, *J. Mol. Biol.* **2002**, *320*, 597.

[19]   D. F. Green, B. Tidor, *J. Phys. Chem., B.* **2003**, *107*, 10261.

[20]   H. Robinson, A. S. Soares, M. Becker, R. Sweet, A. Heroux, *Acta Crystallogr., Sect. D: Biol. Crystallogr.* **2006**, *62*, 1336.

[21]   Z. Otwinowski, W. Minor*, Vol. Volume 276* (Ed.: W. C. Charles, Jr.), Academic Press, **1997**, pp. 307.

[22]   S. Bailey, *Acta Crystallogr., Sect. D: Biol. Crystallogr.* **1994**, *50*, 760.